We analyzed the C I lines associated with the damped Lyα system observed at $z_{\rm abs} = 1.15$ in the spectrum of HE 0515–4414 to derive the ^{12}C/^{13}C ratio. The spectrum was obtained by means of the UV-Visual Echelle Spectrograph (UVES) at the ESO Very Large Telescope (VLT). The obtained lower limit ^{12}C/^{13}C > 80 (2σ C.L.) shows for the first time that the abundance of ^{13}C in the extragalactic intervening clouds is very low. This rules out a significant contribution from intermediate-mass stars to the chemical evolution of matter sampled by this line of sight. The estimated low amount of ^{13}C is in agreement with low abundances of nitrogen observed in damped Lyα systems – the element produced in the same nuclear cycles and from about the same stars as ^{13}C.

Key words. Cosmology: observations – Line: profiles – Stars: nucleosynthesis – Quasars: absorption lines – Quasars: individual: HE 0515–4414

Astronomy & Astrophysics manuscript no. Hi202 February 5, 2008
(DOI: will be inserted by hand later)

VLT/UVES constraints on the carbon isotope ratio $^{12}C/^{13}C$ at $z = 1.15$ toward the quasar HE 0515–4414⋆

S. A. Levshakov[1], M. Centurión[2], P. Molaro[2,3], and M. V. Kostina[4]

[1] Department of Theoretical Astrophysics, Ioffe Physico-Technical Institute, 194021 St. Petersburg, Russia
[2] Osservatorio Astronomico di Trieste, Via G. B. Tiepolo 11, 34131 Trieste, Italy
[3] Observatoire de Paris 61, avenue de l'Observatoire, 75014 Paris, France
[4] Sobolev Astronomical Institute, St. Petersburg State University, 198504 St. Petersburg, Russia

Received 00 / Accepted 00

Abstract.

1. Introduction

The evolution of the chemical composition of matter in the Universe is closely related to the history of star formation and destruction, stellar nucleosynthesis and enrichment of the interstellar/intergalactic medium (ISM/IGM) with processed material. The behavior of the stable CNO isotopes during the cosmic time is of particular interest since their ratios trace the production of *primary* and *secondary* elements[1] which depends on the principal chemical evolution parameters: the stellar initial mass function (IMF), the rate of the mass loss from evolved stars, and the dredge-up episodes leading to the mixture of the surface layers with deeper layers of the star (Wannier 1980; Renzini & Voli 1981; Marigo 2001; Meynet et al. 2005).

^{12}C is a primary product of stellar nucleosynthesis and is formed in the triple-α process during hydrostatic helium burning (van den Hoek & Groenewegen 1997; El Eid 2005). ^{13}C is supposed to have mainly a secondary origin, and is produced in the hydrogen burning shell when the CN cycle converts ^{12}C into ^{13}C (Wannier 1980). However, chemical evolution models considered by Prantzos et al. (1996) match observations better if a mixture of primary+secondary origin in intermediate-mass stars is assumed for ^{13}C. Evolution of massive rotating stars at very low metallicities may also contribute to primary ^{13}C (Meynet et al. 2005). The predicted values for the ratio $\mathcal{R} = ^{12}C/^{13}C$ in the rotationally enhanced winds diluted with the supernova ejects are between 100 and 4000, whereas the ^{13}C yields of massive non-rotating stars are negligible, $\mathcal{R} \sim 3 \times 10^8$. Besides, Meynet et al. show that the rotating AGB and massive stars have about the same effects on the isotope production. The difference between them is only in the isotope composition of the massive star wind material and the AGB star envelopes: the former is characterized by very low values of $\mathcal{R} \sim 3 - 5$, while the latter have $\mathcal{R}$ ranging between 19 and 2500 (the lower $\mathcal{R}$ values correspond to the most massive AGB stars).

Chemical evolution models predict a decrease of the isotope ratio $^{12}C/^{13}C$ with time and an increase with galactocentric distance at a fixed time (Audouze et al. 1975; Dearborn et al. 1978; Tosi 1982; Romano & Matteucci 2003).

For instance, a photospheric solar ratio $\mathcal{R} = 95 \pm 5$ (Asplund et al. 2005), representative of the local ISM 5 billion years ago, is higher than the present value $\mathcal{R} \sim 60-70$ obtained through optical, UV, and IR absorption line observations as well as radio emission line measurements (see, e.g., Hawkins & Jura 1987; Centurión & Vladilo 1991; Centurión et al. 1995; Goto et al. 2003; and references therein). It should be noted, however, that on scales of $\sim$ 100 pc the local ISM is probably chemically inhomogeneous (Casassus et al. 2005) making this difference uncertain.

The high resolution observations ($\lambda/\delta\lambda \gtrsim 50\,000$) of quasar absorption-line spectra available nowadays at large telescopes allow us to probe the isotope composition of the intervening damped Lyα (DLA) systems through the analysis of C I lines, and, hence, to perform an important test of models of stellar nucleosynthesis outside the Milky Way. The most convenient C I transitions are from the $2u$ (λ1657 Å) and $3u$ (λ1561 Å) multiplets (Morton 2003) which cover the redshift range from $z \sim 1$ to $z \sim 3.5$

Send offprint requests to: S. A. Levshakov
lev@astro.ioffe.rssi.ru

⋆ Based on observations performed at the VLT Kueyen telescope (ESO, Paranal, Chile). The data are retrieved from the ESO/ST-ECF Science Archive Facility.

[1] A chemical element is called primary/secondary if its mass fraction ejected from a star is insensitive/ sensitive to the original metallicity of the star (Talbot & Arnett 1974).

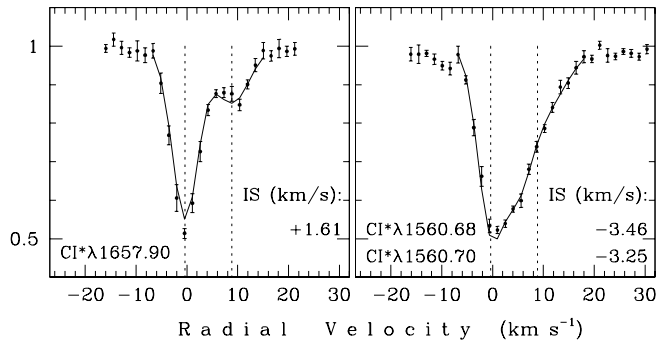

Fig. 1. Normalized intensities (dots with 1σ error bars) of the C I lines selected from the VLT/UVES spectrum of HE 0515–4414. The zero radial velocity is fixed at $z = 1.150789$ (QBR). The over-plotted smooth curves show the best fitted synthetic profiles ($\chi^2_{\rm min} = 1.250$, the number of degrees of freedom $\nu = 26$). The dashed vertical lines mark positions of the C I sub-components. Note that the $\lambda1560$ absorption feature consists of two sub-components with different oscillator strengths: $f_{1560.68} = 0.0581$ and $f_{1560.70} = 0.0193$. The ^{12}C I* oscillator strengths, laboratory vacuum wavelengths and isotopic shifts (IS) are taken from Morton (2003)

(look-back time $\sim 7.7 - 11.8$ Gyr)[2] in optical spectra of distant QSOs.

The analysis of the isotopic composition of the DLA systems is also connected to the interpretation of the hypothetical variation of the fine-structure constant ($\alpha \equiv e^2/\hbar c$) at early cosmological epochs (Ashenfelter et al. 2004a,b; Fenner et al. 2005, hereafter FMG).

In the present letter we report constraints on the carbon isotope abundance in the $z_{\rm abs} = 1.15$ sub-DLA system toward HE 0515–4414 (Reimers et al. 1998). The metallicity of this sub-DLA is found to be lower than solar: [Zn/H] $\simeq -0.99$[3] according to de la Varga et al. (2000), or [Zn/H] $\simeq -0.49$ as measured by Reimers et al. (2003) who revised the H I column density. Sects. 2 and 3 describe the observations and the analysis. The obtained results and their astrophysical implications are discussed in Sect. 4.

2. Observations and data reduction

The observations were acquired with the UV-Visual Echelle Spectrograph (UVES) at the VLT 8.2 m telescope at Paranal, Chile, and the spectral data were retrieved from the ESO archive. The seven selected exposures were described in detail in Levshakov et al. (2005a, hereafter Paper I).

The C I lines analyzed in the present paper are located near the center of the echelle orders. This minimizes possible distortions of the line profiles caused by the decreasing spectral sensitivity at the edges of echelle orders.

Following Paper I, where all details of the data reduction are given, we work with the reduced spectra with the original pixel sizes in wavelength. The residuals of the calibrations give $\sigma_{\rm rms} \lesssim 1$ mÅ. The observed wavelength scale of each spectrum was transformed into vacuum, heliocentric wavelength scale (Edlén 1966). The instrumental profile is dominated in this case by the slit width (0.8 arcsec). The spectral resolution calculated from the narrow lines of the arc spectra is FWHM $= 5.60 \pm 0.10$ km s^{-1}.

After the normalization to the local continuum, the spectra from different exposures were rebinned with the step equal to the mean pixel size. To eliminate instrumental velocity calibration errors, we used the first exposure as a reference frame and calculated residual differences in the radial velocity offsets of other exposures through the cross-correlation analysis. The aligned C I spectra were co-added with weights inversely proportional to $\sigma^2_{\rm cont}$. The resulting average C I profiles are shown in Fig. 1 by dots with 1σ error bars.

3. Analysis

The key points in the study of the isotopic abundance from the UV C I lines are as follows:

1. At high redshift, C I is observed in the most dense and cool sub-components of DLA systems where H_2 lines are usually also detected. The kinetic temperature in such C I-bearing clouds is low. For our particular case $T_{\rm kin} \sim 200$ K (Reimers et al. 2003). It means that the thermal width of the carbon lines is small, $b_{\rm th} \sim 0.5$ km s^{-1}, and the line profiles can be very narrow if the turbulent broadening is not significant.

2. The isotopic shift (IS)[4] between ^{12}C and ^{13}C lines shows different values and signs (Morton 2003). For instance, IS$_{1657.907/1657.916} = 1.61$ km s^{-1}, whereas IS$_{1560.682/1560.664} = -3.46$ km s^{-1}. Although with the spectral resolution of FWHM $= 5.6$ km s^{-1} these lines cannot be completely resolved, the presence of ^{13}C can shift and broaden ^{12}C lines leading to the disparity of line positions from different multiplets. The effect is small when C I lines are optically thin. The centroid of a pair of lines ^{12}C+^{13}C is shifted by $\Delta v = {\rm IS}/(1+\mathcal{R})$ with respect to the position of the ^{12}C line. Suggesting $\mathcal{R} = 60$, this gives for the 1657.907 and 1560.682 lines $\Delta v = +0.026$ and -0.057 km s^{-1}, making the disparity of line positions compared to the assumption of pure ^{12}C equal to 0.083 km s^{-1}. However, the disparity increases with increasing optical depth. For saturated lines with $\tau_0(^{13}{\rm C}) > 1$ and a pure rectangular velocity profile, the short wavelength side of this box-shaped absorption can be displaced by +IS or –IS. The centroid of ^{12}C+^{13}C is then shifted by half of IS, irrespective of $\mathcal{R}$. In this case the disparity is equal to 2.535 km s^{-1}, which already detectable at our resolution. Note that for HE 0515-4414 the line centering can be done with an accuracy better than 1/10 pixel size which

[2] Assuming the cosmological expansion parameterized by $t_0 = 13.8$ Gyr, $h = 0.7$, $\Omega_m = 0.3$, and $\Omega_\Lambda = 0.7$.

[3] [A/B] $\equiv \log(N_{\rm A}/N_{\rm B}) - \log(N_{\rm A}/N_{\rm B})_\odot$.

[4] Defined as IS $= c\,(\lambda_{13} - \lambda_{12})/\lambda_{12}$ (in km s^{-1}).

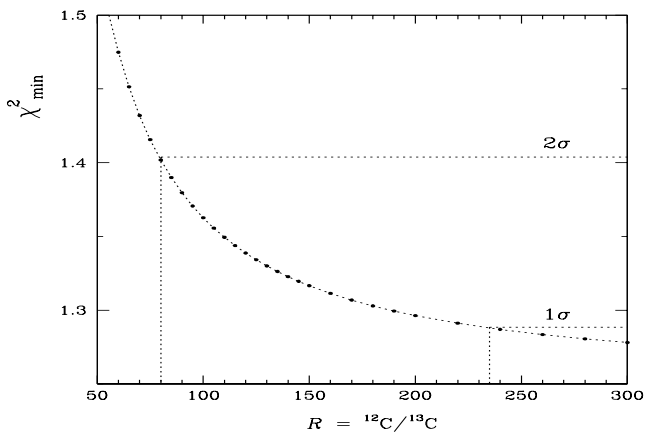

Fig. 2. Confidence intervals in the "χ^2-$\mathcal{R}$" plane calculated from the simultaneous fit of the C I* lines shown in Fig. 1.

is about 150 m s^{-1} (Paper I). Since the strengths of carbon lines from the UV multiplets cover a wide dynamical range, the saturation effects can be correctly taken into account.

3. Since the atomic carbon isotopic abundance seems to be unaffected by depletion, the measured ratio $^{12}C/^{13}C$ reflects the carbon isotopic ratio at a given redshift.

The VLT/UVES spectrum of HE 0515–4414 reveals multi-component C I profiles at $z_{abs} = 1.15$ (Fig. 1). Their diagnostic was performed by de la Varga et al. (2000) and later by Quast et al. (2002, hereafter QBR). All C I lines are well described by a two-component Voigt profile model (see Fig. 1 in QBR). Besides, QBR found that the subcomponents of the C I lines arising from the $J = 0, 1$, and 2 levels of the ground state have different relative strengths indicating inhomogeneous physical conditions in the C I-bearing cloud.

The heterogeneity of the absorbing medium may cause small relative velocity shifts between C I transitions with different J similar to the shifts observed between H_2 lines in the direction of ζ Ori A (Jenkins & Peimbert 1977). This would add an additional noise in the measurements of the disparity of the C I line positions. To avoid this putative effect we selected from the observed eight C I lines (QBR) only two $J = 1$ transitions which show most pronounced isotopic shifts. These are just the lines C I* λ1560.68 and λ1657.90 mentioned above. Other C I* lines (λ1656.26 and λ1657.37), as well as the lines with $J = 0$ and 2 are less sensitive to the presence of ^{13}C since their isotopic shifts are smaller than those of λ1560.68 and λ1657.90.

Following QBR, we use two-component model to constrain the isotope ratio $\mathcal{R}$ from the minimization of the objective function defined by eq.(2) in Paper I. The χ^2_{min} values (normalized per degree of freedom) are calculated in the interval $30 \le \mathcal{R} \le 3000$ and shown as a function of $\mathcal{R}$ in Fig. 2. This function gradually decreases with increasing $\mathcal{R}$ and tends to a limit $\chi^2_{lim} = 1.250$ at $\mathcal{R} \gg 1$. This global minimum $\chi^2_{lim} = 1.250$ lies within 1σ uncertainty range since at $\nu = 26$ the expected mean value of χ^2_ν is equal to 1 ± 0.277. The optimized values and formal uncertainties of the model parameters for both C I* absorption components (labeled by subscripts '1' and '2') at zero ^{13}C abundance are as follows: the column density $N_1 = (3.5 \pm 0.3) \times 10^{13}$ cm^{-2}, $N_2 = (6.3 \pm 0.4) \times 10^{12}$ cm^{-2}, the Doppler parameter $b_1 = 1.10 \pm 0.06$ km s^{-1}, $b_2 = 3.40 \pm 0.17$ km s^{-1}, and the radial velocity difference $\Delta v_{2-1} = 9.23 \pm 0.28$ km s^{-1}. The corresponding synthetic profiles are shown in Fig. 1 by smooth curves. The model parameters do not change for $\mathcal{R} > 300$.

The dashed horizontal lines in Fig. 2 mark the 1σ and 2σ confidence levels. Since the curve $\chi^2_{min}(\mathcal{R})$ is almost flat at $\mathcal{R} > 300$, the present data allow us to constrain only the lower limits on the carbon isotopic ratio: $\mathcal{R} > 235$ (1σ C.L.), or a more conservative restriction $\mathcal{R} > 80$ (2σ C.L.). The former value is, however, less certain due to a small gradient of the $\chi^2_{min}(\mathcal{R})$ function at large $\mathcal{R}$.

We also used a 3-component model to test robustness of the obtained results. Being applied to the lines of C I $\lambda\lambda$1560.3, 1658.9, C I* $\lambda\lambda$1560.7, 1657.9, and C I** $\lambda\lambda$1561.3, 1657.0, 1658.1 this model yields $\mathcal{R}_{1\sigma} > 145$ and $\mathcal{R}_{2\sigma} > 78$ with $\chi^2_{min} = 1.020$ ($\nu = 93$) at $\mathcal{R} \gg 1$. The concordance of all available C I profiles is demonstrated in Fig. 3.

4. Discussion and Conclusions

We re-analyzed the profiles of the C I lines associated with the sub-DLA system observed at $z_{abs} = 1.15$ in the spectrum of HE 0515–4414. Our main purpose was to set a constraint to the carbon isotopic abundance outside the Milky Way, in distant intervening clouds at the cosmological epoch corresponding to 8.2 Gyr of the look-back time. Similar tasks were discussed by Carlsson et al. (1995), Labazan et al. (2005), and FMG.

The present $\Delta\chi^2$ analysis gives $^{12}C/^{13}C > 80$ (2σ C.L.). This low abundance of ^{13}C does not support the enrichment of gas by the wind from rotating massive stars (Meynet et al. 2005). Besides, it can constraint the fraction of intermediate-mass (IM) stars ($4 \lesssim M/M_\odot \lesssim 8$) in the IMF. For instance, the FMG models for the chemical evolution of the Galaxy with normal IMF attain the solar ratio $^{12}C/^{13}C \simeq 90$ already at [Fe/H] ≈ -2 for the outer radius and [Fe/H] ≈ -1.5 for the solar radius case, respectively. On the contrary, the models with an enhanced population of IM stars produce oversolar abundances of ^{13}C at all metallicities [Fe/H] < -0.3 (cf. Fig. 9 in FMG). Thus, these models can be ruled out by our measurements.

Closely related to $^{12}C/^{13}C$ ratio is the problem of nitrogen, ^{14}N, which is expected to be produced in the same way and from about the same stars as ^{13}C. Measurements in DLAs show very low N abundances which is consistent with the absence of an enhanced population of IM stars to the chemical evolution of the gas (Centurión et al. 2003). Thus, low ^{13}C and low ^{14}N seem to be in agreement.

It should be noted, however, that the chemical evolution of nitrogen is still not well understood since the existing models predict abundances higher than observed in DLAs (see, e.g., Fig. 6 in FMG).

The present bound to the abundance of ^{13}C and, as a result, to the contribution of the AGB stars to the chemical evolution of the $z_{abs} = 1.15$ system may be indirectly related to the claims of a possible time variation of the fine-structure constant, α (see Murphy et al. 2004 and references therein). A significant portion of the sample used by Murphy et al. involves the comparison of Mg II and Fe II wavelength shifts. Later on, it was shown that over-solar abundances (~ 0.3 dex) of $^{25,26}Mg$ isotopes with respect to ^{24}Mg in the absorbing material can imitate an apparent variation of α in the redshift range between 0.5 and 1.8 (Ashenfelter et al. 2004a,b). The production of Mg isotopes is believed to occur in about the same stars which produce ^{13}C. Thus, the obtained bound to the amount of ^{13}C, taken as a typical value for the DLA systems[5], poses a limit to the role of the AGB stars in mimicking the α variations. However, the variability of α has not been supported by more recent studies (Quast et al. 2004; Chand et al. 2004; Levshakov et al. 2005a,b). This may suggest the presence of other systematic errors to explain the different results concerning the variability of α.

Acknowledgements. The authors thank Edward Jenkins and Ralf Quast for useful comments. This work is supported by the RFBR Grant No. 03-02-17522 and by the RLSS Grant No. 1115.2003.2.

References

Ashenfelter, T. P., Mathews, G. J., & Olive, K. A. 2004a, Phys. Rev. Lett., 92, 041102
Ashenfelter, T. P., Mathews, G. J., & Olive, K. A. 2004b, ApJ, 615, 82
Asplund, M., Grevesse, N., & Sauval, J. A. 2005, in Cosmic Abundances as Records of Stellar Evolution and Nucleosynthesis, ed. F. N. Bash & T. G. Barnes, in press (astro-ph/0410214)
Audouze, J., Lequeux, J., & Vigroux, L. 1975, A&A, 43, 71
Carlsson, J., Jönsson, P., Godefroid, M. R., & Froese Fische, C. 1995, J. Phys. B, 28, 3729
Casassus, S., Stahl, O., & Wilson, T. L. 2005, A&A, 441, 181
Centurión, M., Molaro, P., Vladilo, G., Péroux, C., Levshakov, S. A., & D'Odorico, V. 2003, A&A, 403, 55
Centurión, M., Càssola, C., & Vladilo, G. 1995, A&A, 302, 243
Centurión, M., & Vladilo, G. 1991, A&A, 251, 245
Chand, H., Srianand, R., Petitjean, P., & Aracil, B. 2004, A&A, 417, 853
Dearborn, D., Tinsley, B. M., & Schramm, D. N. 1978, ApJ, 223, 557
de la Varga, A., Reimers, D., Tytler, D., Barlow, T., & Burles, S. 2000, A&A, 363, 69
Edlén, B. 1966, Metrologia, 2, 71
El Eid, M. 2005, Nature, 433, 117
Fenner, Y., Murphy, M. T., & Gibson, B. K. 2005, MNRAS, 358, 468 [FMG]
Goto, M., Usuda, T., Takato, N. et al. 2003, ApJ, 598, 1038
Hawkins, I., & Jura, M. 1987, ApJ, 317, 926
Jenkins, E., & Peimbert, A. 1977, ApJ, 477, 265
Labazan, I., Reinhold, E., Ubachs, W., & Flambaum, V. V. 2005, Phys. Rev. A, 71, 040501
Levshakov, S. A., Centurión, M., Molaro, P., et al. 2005a, A&A, in press (astro-ph/0511765) [Paper I]
Levshakov, S. A., Centurión, M., Molaro, P., & D'Odorico, S. 2005b, A&A, 434, 827
Marigo, P. 2001, A&A, 370, 194
Meynet, G., Ekström, S., & Maeder, A. 2005, A&A, in press (astro-ph/0510560)
Morton, D. C. 2003, ApJS, 149, 205
Murphy, M. T., Flambaum, V. V., Webb, J. K., et al. 2004, in Astrophysics, Clocks and Fundamental Constants, ed. S. G. Karshenboim & E. Peik (Springer-Verlag, Berlin) 131
Prantzos, N., Aubert, O., & Audouze, J. 1996, A&A, 309, 760
Prochaska, J. X. 2003, ApJ, 582, 49
Quast, R., Reimers, D., & Levshakov, S. A. 2004, A&A, 415, L7
Quast, R., Baade, R., & Reimers, D. 2002, A&A, 386, 796 [QBR]
Reimers, D., Baade, R., Quast, R., & Levshakov, S. A. 2003, A&A, 410, 785
Renzini, A., & Voli, M. 1981, A&A, 94, 175
Romano, D., & Matteucci, F. 2003, MNRAS, 342, 185
Talbot, R. J., & Arnett, D. W. 1974, ApJ, 190, 605
Tosi, M. 1982, ApJ, 254, 699
van den Hoek, L. B., & Groenewegen, M. A. T. 1997, A&AS, 123, 305
Wannier, P. G. 1980, ARA&A, 18, 399

[5] The DLA population shows a remarkable similarity in the relative chemical abundances (Prochaska 2003).

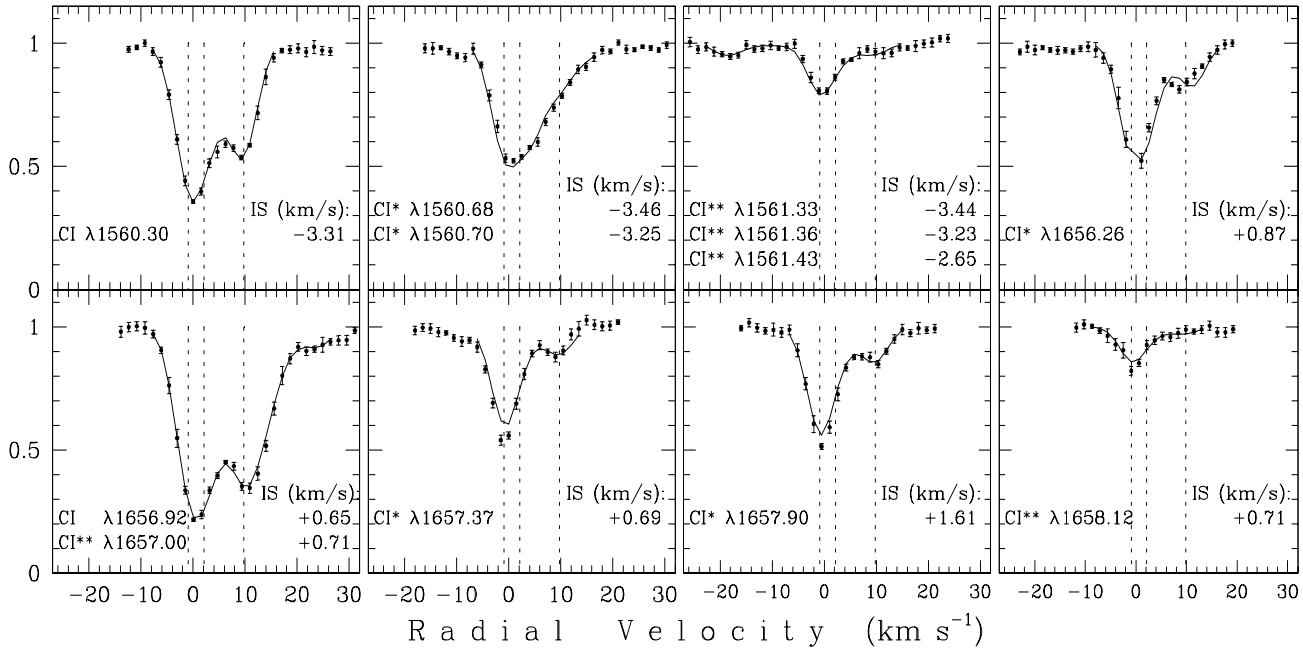

Fig. 3. Same as Fig. 1 but for a 3-component Voigt profile model fitted to all available C I lines. The over-plotted smooth curves show the best fitted synthetic profiles ($\chi^2_{\rm min} = 1.036$, the number of degrees of freedom $\nu = 125$). The dashed vertical lines mark positions of the C I sub-components